Drug Design of Anti-metastatic Agents

Targeting Tumor Hypoxia

腫瘍低酸素を標的とする抗転移剤の薬剤設計

2018 年　3 月

芝　一休

Contents

Chapter 2: Design and Synthesis of Novel Anti-metastatic Hypoxic Cytotoxin Based on 2,3-Diphenylquinoxaline

Chapter 1: Design and Synthesis of Novel Anti-metastatic Hypoxic Cytotoxin TX-2137 Targeting AKT Kinase

1.Abstract

Background: The hypoxic microenvironment plays a crucial role in malignant progression of tumor cells. Moreover, AKT, a serine/threonine kinase, is activated by various extracellular growth factors and is important for cell growth, survival, and motility of leukocytes, fibroblasts, endothelial cells, and tumor cells. Therefore, we aimed to design an anti-metastatic hypoxic cytotoxin which has inhibitory effect on AKT.

Result: TX-2137 was designed and synthesized based on the structural similarity of a preexisting AKT1/2 kinase inhibitor and a hypoxic cytotoxin tirapazamine. TX-2137 effectively reduced the expression of phosphorylated AKT and matrix metalloproteinase 9 (MMP9) and showed strong inhibition of the proliferation of B16-F10, HT-1080, and MKN-45 cells. In addition, TX-2137 exhibited hypoxia-selective cytotoxicity towards A549 cells and inhibited liver metastasis of B16-F10 cells in a xenograft chick embryo model in the same way as doxorubicin.

Conclusion: TX-2137 may be a potent lead compound in the development of a novel anti-metastatic AKT kinase inhibitor.

2. Introduction

Hypoxia, a characteristic feature of many solid tumors, leads to chemoresistance, radioresistance, increased angiogenesis, vasculogenesis, invasion, metastasis, resistance cell death, genomic instability, and changes in metabolism (1-6) (Figure 1). Tirapazamine (SR 4233) is a well-known drug that specifically exerts toxicity under such hypoxic conditions through the release of free radicals (7, 8). These free radicals, formed by natural decay of oxidized hydroxyl radical ($OH^{\cdot}$) or benzotriazinyl radical ($BTZ^{\cdot}$) following one-electron reduction of tirapazamine by NADPH-cytochrome 450 reductase, induce cytotoxicity by causing double-strand breakage of DNA (9). Tirapazamine is a prodrug that has advanced to phase III clinical trials (10, 11) (Figure 2). A phase III clinical trial was conducted in patients with head and neck cancer with tirapazamine in combination with radiation or chemoradiation with cisplatin, but no significant differences in the 2-year overall survival and failure-free survival were reported when compared with patients treated with radiation plus cisplatin (12). However, the tirapazamine combination treatment with radiation plus cisplatin was effective when compared with chemoradiation with cisplatin and fluorouracil (10). The tirapazamine combination treatment is still feasible and its clinical trials are ongoing in patients with locally advanced cervical cancer and oropharyngeal cancer (NCT00094081, NCT00262821).

The phosphoinositide 3-kinase (PI3K)/AKT signal pathway is the most frequently activated signal transduction pathway in human cancer (13) and plays an important role in the cell cycle regulation, survival, migration, invasion, and metastasis of cancer cells (14-16) (Figure 3). In addition, Young *et al.* reported that activated AKT accumulates in mitochondria under hypoxic conditions; changes various cellular responses and biological processes such as tumor metabolism to glycolytic system, apoptosis, and resistance to autophagy; alleviates oxidative stress, and maintains the growth of tumor cells faced with severe hypoxia (17). In this study, I, therefore, designed and synthesized an anti-metastatic hypoxic cytotoxin with AKT-inhibitory activity.

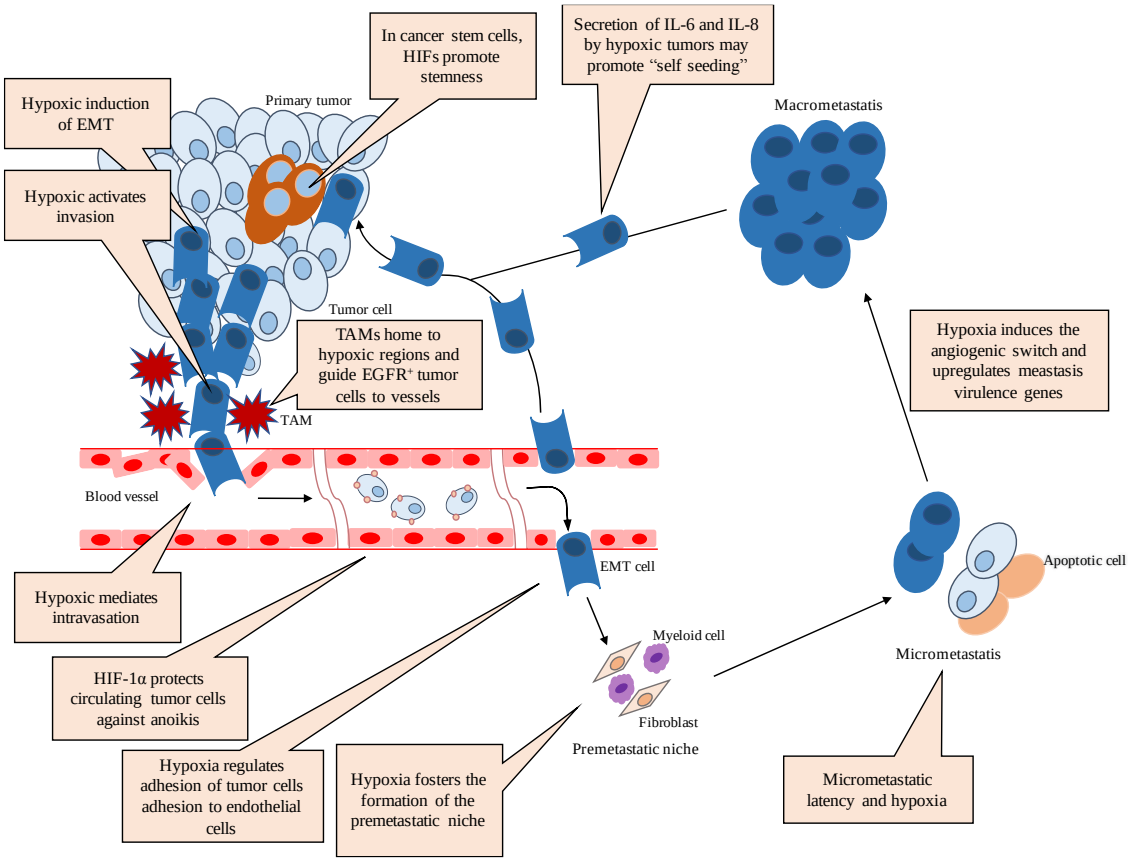

Figure 1. Metastatic cascade and its regulation by hypoxia. Original figure was cited in Nature Reviews Clinical Oncology 31: 393-404, 2011.

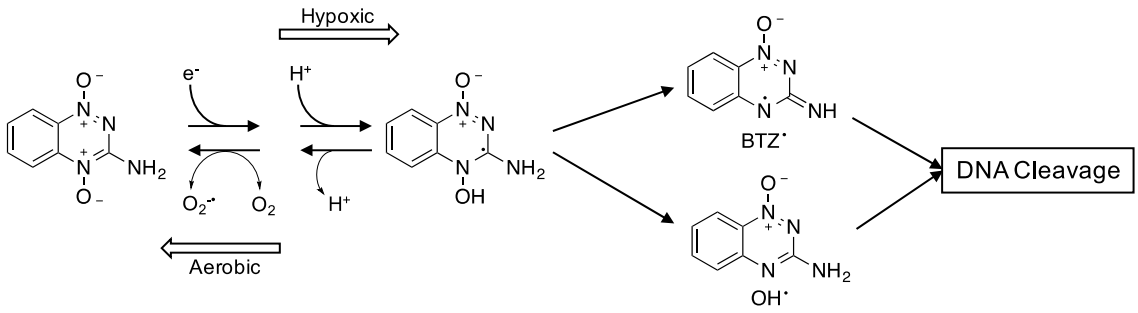

Figure 2. Mechanism of hypoxic cytotoxicity of Tirapazamine.

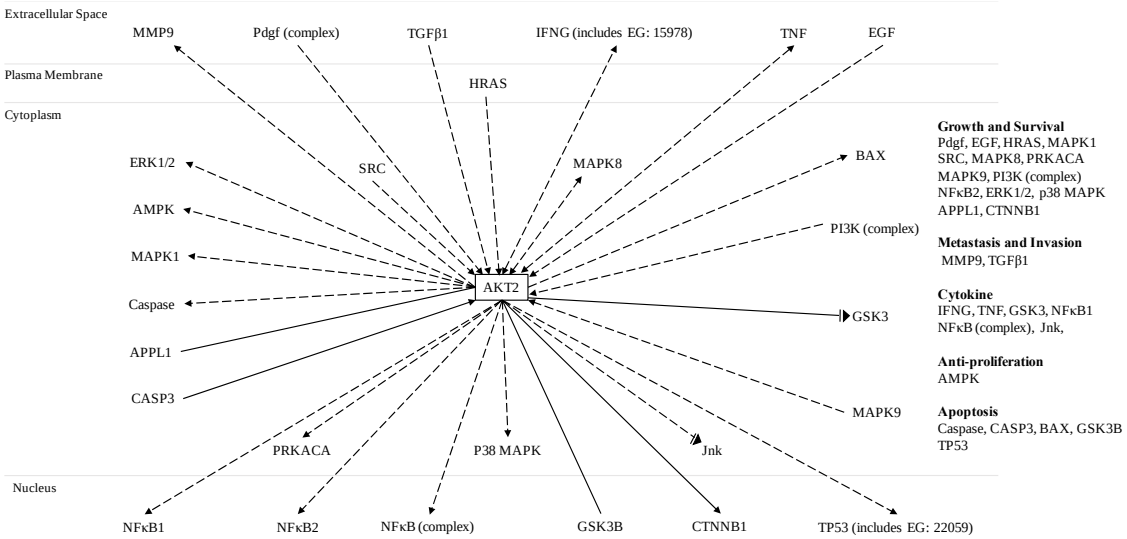

Figure 3. Predicted mRNA targets of AKT2 in the context of colorectal cancer metastasis signaling. Original Figure was cited in Cellular Signaling 25: 1711-1719, 2013.

3. Materials and Methods

3-1. Materials

Reagents and solvents were purchased from standard suppliers and used without further purification unless otherwise indicated. ^{1}H nuclear magnetic resonance (NMR) spectra were obtained using a JNM-EX400 spectrometer (JEOL, Tokyo, Japan) at 400 MHz. Solvents were evaporated under reduced pressure on a rotary evaporator. Thin-layer chromatography was performed on glass-backed silica gels (Merck 60 F254; Merck Japan, Tokyo, Japan) and components were visualized using ultraviolet (UV) light. Column chromatography was performed using a silica gel (60 N, spherical neutral; 40-50 μm; KANTO Chemical, Tokyo Japan). The molecular orbital structure was calculated by WinMOPAC 3.0 (PM3, Fujitsu, Kawasaki, Japan).

3-2. Cell culture

B16-F10 mouse melanoma cells (kindly provided by Dr. Tsuruo, Tokyo University, Tokyo, Japan) and A549 human lung carcinoma cells (supplied by Dr. Kondo, Kyoto University, Kyoto, Japan) were maintained in Dulbecco's modified Eagle's medium (DMEM), while HT-1080 human sarcoma cells (purchased from American type culture collection, Manassas, VA, USA) were cultured in Eagle's minimum essential medium (EMEM). MKN-45 human adenocarcinoma cells (Dr. Suzuki, Fukushima Medical College, Fukushima, Japan) and U87MG human neuronal glioblastoma cells (American Type Culture Collection Manassas, VA, USA) were maintained in RPMI-1640 medium. All media were supplemented with 10% fetal bovine serum and cells were cultured in a humidified atmosphere of 5% CO_2 at 37˚C. Hypoxic culture was performed in a humidified atmosphere of 0.1% O_2 at 37˚C using an AnaeroPack (Mitsubishi Gas Chemical, Tokyo, Japan).

3-3. Synthesis of 3-chloro-1,2,4-benzotriazine 1-oxide

2-Nitroaniline (10 g, 72.4 mmol) and cyanamide (6.0 g, 144.8 mmol) were melted at 100 °C. Thereafter, 36% hydrochloric acid (HCl) (40 mL) was slowly added and the mixture was stirred at 100 °C for 2 h then the solution was cooled to room temperature. To this mixture, 7.5 M aqueous NaOH solution (200 mL) was slowly added and stirred at 100 °C for 2.5 h. Finally, the solution was cooled to room temperature and water (200 mL) was added and a substance precipitated from the solution was filtered with filter paper to yield compound **1** (3-amino-1,2,4-benzotriazine 1-oxide) as a yellow solid (18). 3-Amino-1,2,4-benzotriazine 1-oxide was dissolved in trifluoroacetic acid (TFA) (60 mL) at 5 °C and sodium nitrite (4.8 g, 71.4 mmol) was added. The solution was stirred at room

temperature for 2 h and was added dropwise to ice/water. The precipitate was collected, washed with water, and dried. The solid produced (compound **2**; 3-hydroxy-1,2,4-benzotriazine 1-oxide) was suspended in phosphoryl chloride ($POCl_3$) (27 mL) and *N,N*-dimethylformamide (DMF) (5.0 mL) and stirred at 100 °C for 1 h. Once cooled, the solution was added dropwise to ice/water, the precipitate was collected, washed with water, and dried. The precipitate was purified by silica-gel column chromatography with dichloromethane (CH_2Cl_2) to give compound **3** (3-chloro-1,2,4-benzotriazine 1-oxide) (1.9 g, 14.8% yield) (19).

3-4. Synthesis of TX-2137

4-Aminophenol (1.0 g, 9.2 mmol) and imidazole (1.2 g, 18.3 mmol) were suspended in CH_2Cl_2 under a nitrogen atmosphere. *tert*-Butylchlorodimethylsilane (TBDMSCl) (2.1 g, 13.7 mmol) was added and the solution was stirred at room temperature for 1 h, poured into Brine and extracted with CH_2Cl_2. The organic layer was evaporated to give compound **4** (1.5 g, 73.1% yield). Next, compound **4** (0.25 g, 1.1 mmol) was dissolved in CH_2Cl_2. Triethylamine (Et_3N) (156 μl, 1.1 mmol) and 3-chloro-1,2,4-benzotriazine 1-oxide (0.1 g, 0.6 mmol) were added and the solution was stirred at room temperature for 2 h, poured into water and extracted with CH_2Cl_2. The organic layer was evaporated and purified by silica-gel column chromatography with CH_2Cl_2 to give compound **5** (0.17 g, 84.1% yield). Next, compound **5** (0.1 g, 0.27 mmol) and $NaHCO_3$ (45 mg, 0.54 mmol) were dissolved in CH_2Cl_2. *m*-Chloroperoxybenzoic acid (*m*-CPBA) (93 mg, 0.54 mmol) was added and the mixture stirred at room temperature for 24 h. The solution was collected using a filter paper, the filtrate was evaporated and the residue was purified by silica-gel column chromatography with 20%-methanol (MeOH) / ethyl acetate (EtOAc), forming compound **6** (62 mg, 54.9% yield). Finally, compound **6** (0.61 g, 1.6 mmol) was dissolved in tetrahydrofuran (THF) at 5 °C and 1.0 M of tetrabutylammonium fluoride (TBAF) solution (3.2 mL, 3.2 mmol) was added. The solution was stirred at room temperature for 5 min, solvents were evaporated and the residue was purified by silica-gel column chromatography with 10%-MeOH/EtOAc to obtain compound **7** (TX-2137) (0.37 g, 84.7% yield) as a purple powder; ^{1}H NMR [$(CD_3)_2SO$] δ 9.96 (*s*, 1H, PhOH), 9.41 (*s*, 1H, PhNH), 8.22 (*t*, *J* = 8.5 Hz, 2H), 7.97 (*td*, *J* = 7.8, 1.4 Hz, 1H), 7.61 (*td*, *J* = 7.8, 1.4 Hz, 1H), 7.38 (*d*, *J* = 8.7 Hz, 2H), 6.79 (*d*, *J* = 8.7 Hz, 2H); MS (EI) m/z 270 (M^+, 13), 254 (68), 238 (56), 210 (100); Anal. calcd. for $C_{13}H_{10}N_4O_3$: C, 57.78; H, 3.73; N 20.73. Found C, 57.56; H, 3.76; N, 20.75.

3-5. *In vitro* WST-8 assay to evaluate the effect of TX-2137 on cell proliferation

In vitro cell proliferation was examined using a colorimetric assay with Cell Counting Kit-8 (Dojindo Laboratories, Kumamoto, Japan) according to the manufacturer's instructions. Briefly, B16-F10, HT-1080 and MKN-45 cells were seeded at a density of 5.0×10^3 cells/well in a 96-well plate and TX-2137, dissolved in dimethyl sulfoxide, was added to the culture medium at concentrations between 0.1-100 μM. After 72 h incubation, the medium was replaced with fresh medium containing the WST-8 reagent. After 3 h, the absorbance in each well was determined at 450 nm (with a reference wavelength of 620 nm) using an ImmunoMini NJ-2300 microplate spectrophotometer (BioTec, Tokyo, Japan, Tokyo, Japan). The percentage of cell growth inhibition was calculated by applying the following formula: % of cell growth inhibition = (1-[T/C]) × 100, where C and T were the mean absorbances of the control group and treated group, respectively. The 50% inhibitory concentration (IC_{50}) value was measured graphically from the dose–response curve with at least three drug concentration points.

3-6. *In vitro* hypoxia-selective cytotoxicity of TX-2137 using WST-1 assay

A549 cells were seeded in two 96-well plates at a density of 3×10^3 cells/well and incubation for 24 h. After 24 h, TX-2137 was added at the final concentrations of 0.1 to 30 μM and each plate was incubated either normoxic (21% O_2) or hypoxic (0.1% O_2) conditions for 24 h. After 24 h, each well was washed with 1×PBS and fresh medium containing the WST-1 reagent (Wako Pure Chemical) was added. The absorbance was measured at a wavelength of 450 nm using a Tecan Infinite M200 microplate reader (Tecan, Männedorf, Switzerland).

3-7. AKT inhibition by TX-2137 by western blot analysis on U87MG cells

The harvested cells were homogenized in RIPA buffer (Thermo Scientific, IL, USA) supplemented with protease inhibitors (cOmplete™, Mini, EDTA-free®, Roche Applied Science Tokyo, Japan). After 5 min of centrifugation at 13000 x g, the protein concentration in the supernatant was assayed with BCA reagent (PIERCE, Tokyo, Japan). After reduction in 60 mM Tris-HCl buffer (pH 6.8) containing 10% glycerol, 2% sodium dodecyl sulfate (SDS), 100 mM dithiothreitol (DTT) and 0.002% bromophenol blue, 50 μg of protein were separated by SDS-Poly- Acrylamide Gel Electrophoresis (SDS-PAGE) and transferred to polyvinylidene fluoride (BIO-RAD, Hercules, CA, USA) membranes. The membranes were immersed for 1 h in blocking buffer [5% non-fat dry milk or 5% bovine serum albumin (BSA) in tris-buffered saline (TBS)] and then incubated with primary antibodies to AKT1, AKT2, AKT3 (1:1000; Cell Signaling, Danvers, MA, USA), or phospho-AKT (Ser473) (1:2000; Cell Signaling in Can Get Signal Solution 1 (TOYOBO, Osaka, Japan). The membranes were subsequently

incubated with horseradish peroxidase-conjugated secondary antibodies in Can Get Signal Solution 2 (dilution 1:3000; TOYOBO). The protein–antibody complexes were detected with Amersham ECL® plus (GE Healthcare, Little Chalfont, Buckinghamshire, UK) using a Lumino image analyzer (Image Quant LAS4000 mini; GE Healthcare) and NIH ImageJ 1.46 software (http://rsb.info.nih.gov/ij/). Each experiment was repeated three times.

3-8. Assay of MMP9 inhibition by TX-2137 by gelatin zymography

To analyze the effect of TX-2137 on the activation of pro-MMP2 into its activated form which is induced by MT1-MMP and on the expression and secretion of MMP2 and MMP9, HT1080 cells (5 x 10^4 cells/ml) were seeded into a 48-well culture plate and cultured in 100 µl of complete media for 24 h. After washing twice with serum-free DMEM, the cells were further cultured in OPTI-MEM (Invitrogen) with various concentrations of TX-2137 for 3 h. Then, an aliquot of conditioned medium was analyzed by gelatin zymography. Zymography was performed with an 10% SDS-polyacrylamide gel containing 0.1% gelatin as described previously (20). After electrophoresis, SDS was replaced by Triton X-100, followed by overnight incubation in Tris-based buffer. Gels were stained with Coomassie Brilliant Blue, and gelatinolytic activity of MMP2 and MMP9 was detected as clear bands in the background of uniform staining.

3-9. *In vivo* anti-metastatic activity of TX-2137 using chick embryo model

Fertilized chicken eggs (Plymouth Rock × White Leghorn) were obtained from the Goto Chicken Farm (Gifu, Japan). The assay was performed as originally described by Endo *et al.* (21). Briefly, 5×10^4 cells were injected into the chorioallantoic membrane (CAM) veins of the chicken egg with a 30G needle 11 days after fertilization and eggs were incubated for a further 3 days. TX-2137 (in 0.1 ml) or doxorubicin (Kyowa Hakko Kirin, Tokyo, Japan) was administered into the CAM vein. Doses were as follows: 40 µg/egg for doxorubicin, 62.5 µg/egg and 125 µg/egg for TX-2137. After drug administration, eggs were incubated for another 4 days. Embryo livers were then dissected 7 days after tumor cell injection, and the total DNA was extracted. A fragment of mouse ß-globin gene in the oncogene-transformed cells that colonized liver tissue was amplified by 25 cycles of polymerase chain reaction (PCR) using species-specific primers. Each PCR cycle consisted of 1 min of denaturing at 94°C, 1 min of annealing at 50°C, and 1.5 min of extension at 72°C. The amplified fragment (633 base pairs) was separated by electrophoresis in a 1.2% agarose gel. The signal intensity of the band in agarose gel was measured using image processing program Image J. Oligonucleotide primers were as follows: sense primer *Mgp1* (5'-GGA TCA GTT GCT CCT ACA TT-3') and antisense primer *Mgp5*

(5'-TAT CCG AAC TCT TGT CAA CA-3').

3-10. Statistical analysis

Data are expressed as the mean and standard deviations of at least three independent experiments. The statistical significance of the differences between the results was analyzed using Student's *t*-test. A $p<0.05$ was considered statistically significant.

4. Results

4-1. Design and Synthesis of TX-2137

I focused on the structural similarity of pre-existing AKT1/2 inhibitor and tirapazamine, found in the bicyclic on tirapazamine and tricyclic heteroaromatic ring of AKT1/2 inhibitor as shown by dot lines (Figure 4). I designed the simplified compound TX-2137 by removing the 1-(4-piperidyl)-2-benzimidazolinone moiety of the lead compound of the AKT1/2 inhibitor (22). 3-Chloro-1,2,4-benzotriazine 1-oxide was synthesized using the method described by Pchalek *et al.* (19). Using 4-aminophenol as the starting material, the phenolic hydroxyl group was protected with *tert*-butylchlorodimethylsilane and coupled with 3-chloro-1,2,4-benzotriazine 1-oxide. Thereafter, the N-4 position was oxidized to dioxide and deprotected to obtain TX-2137 (Figure 5).

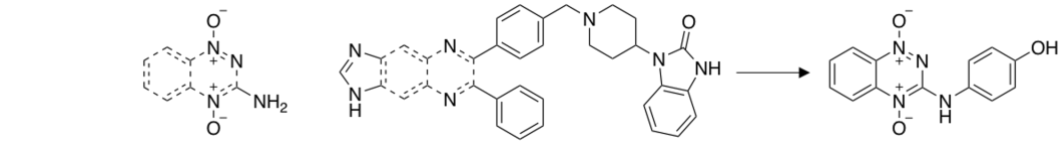

	Tirapazamine	AKT1/2 inhibitor	TX-2137
LUMO (eV)	-1.4041	-0.9709	-1.5026
HOMO (eV)	-8.1342	-8.7148	-7.9846

Figure 4. Design of TX-2137 based on tirapazamine and AKT1/2 inhibitor.

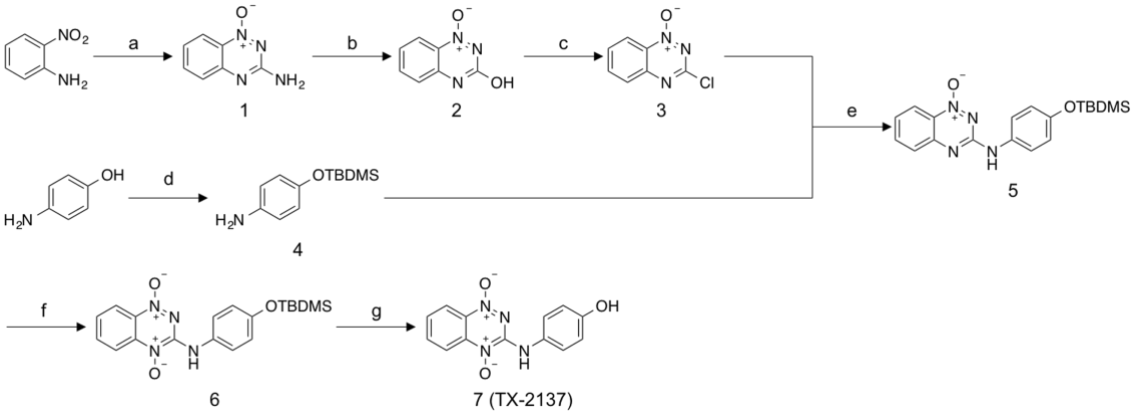

Figure 5. Synthesis of the TX-2137. Reagents: a: Cyanamide, HCl, 7.5 M aquesou NaOH solution; b: TFA, sodium nitrite; c: $POCl_3$, DMF; d: TBDMSCl, imidazole, CH_2Cl_2; e: Et_3N, CH_2Cl_2; f: *m*-CPBA, $NaHCO_3$, CH_2Cl_2; g: 1.0 M-TBAF, THF.

4-2. Cell proliferation-inhibitory activity and hypoxic cytotoxicity of TX-2137

I first evaluated anti-proliferative activity and hypoxia-selective cytotoxicity of TX-2137 in different tumor cells (Table I). Table IA shows the cell proliferation-inhibitory activity of TX-2137 that exhibited a strong anti-proliferative effect against all the tumor cell lines tested. Table IB shows the results of the cytotoxicity assay under normoxic and hypoxic conditions. TX-2137 showed hypoxia-preferential cytotoxicity against A549 cells but the hypoxia selectivity of TX-2137 (4.2-fold) was lower than that of tirapazamine (13.1-fold).

Table I. Cell Proliferation Inhibitory Activity (A) and Hypoxic Cytotoxicity (B) of TX-2137.

A

Compound	IC_{50} (μM)		
	B16-F10	HT-1080	MKN-45
TX-2137	3.7	2.1	1.8

B

Compound	IC_{50} (μM) A549		Hypoxic selectivity, normoxia/hypoxia
	Normoxia	Hypoxia	
TX-2137	9.2	2.2	4.2
Tirapazamine	94.4	7.2	13.1

4-3. AKT-inhibitory activity of TX-2137 on U87MG cells

I evaluated the inhibitory activity of TX-2137 on AKT protein expression, its phosphorylation and cell viability (Figure 6). TX-2137 effectively down-regulated the expression of AKT2 and the phosphorylation of AKT (Figure 6A-C). TX-2137 reduced cell viability by about 50% at 10 μM after 24 and 72 h (Figure 6D). This result correlates with the inhibition of AKT2 expression and AKT phosphorylation by TX-2137.

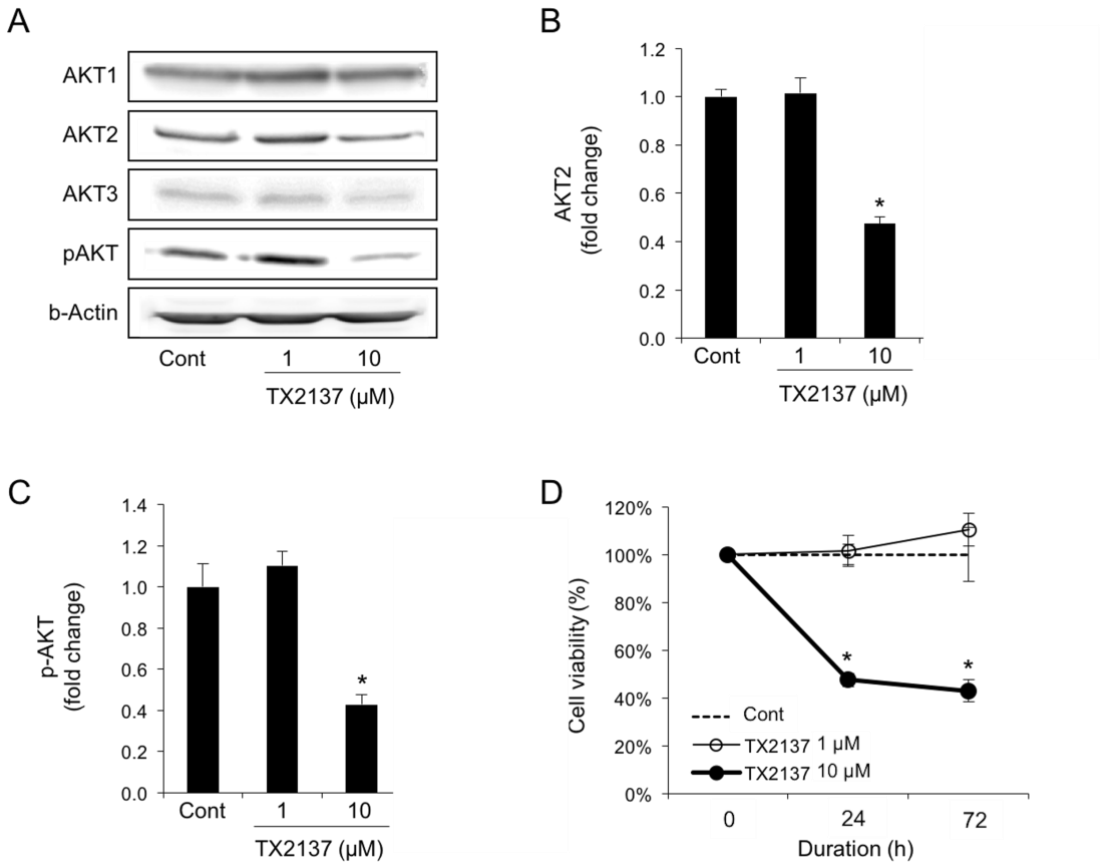

Figure 6. AKT inhibition assay of TX-2137 by western blot analysis and the cell viability in U87MG cells. Each experiment was performed four times, and the data represent the mean ± SD (*$p < 0.05$). A: Western blot analysis to detect AKT protein expression in U87MG cells. Quantitative analysis using Image J (B, C) and the effect of TX-2137 on the cell viability of U87MG (D).

4-4. Inhibitory activity of TX-2137 on MMP9 production in HT-1080 cells

The inhibitory activity of TX-2137 on MMP9 production was evaluated by zymographic assay using HT-1080 cells. TX-2137 inhibited the production of MMP9 but did not alter MMP2 production and activation (Figure 7).

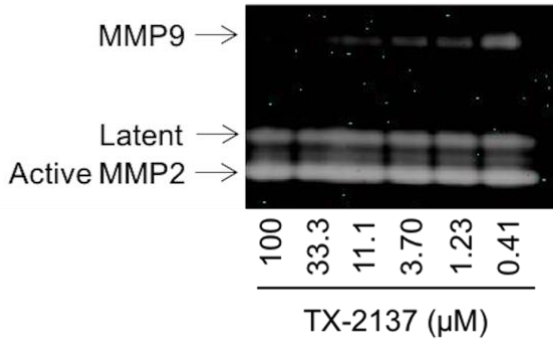

Figure 7. Effect of TX-2137 on matrix metalloproteinase 2 (MMP2) and MMP9. TX-2137 clearly inhibited expression of MMP9 in a concentration-dependent manner.

4-5. Anti-metastatic activity of TX-2137 using chick embryo model on B16-F10 cells

Anti-metastatic activity of TX-2137 was assayed using a xenograft model using chick embryo. TX-2137 effectively prevented liver metastasis of B16-F10 melanoma cells in the same way as doxorubicin (Figure 8).

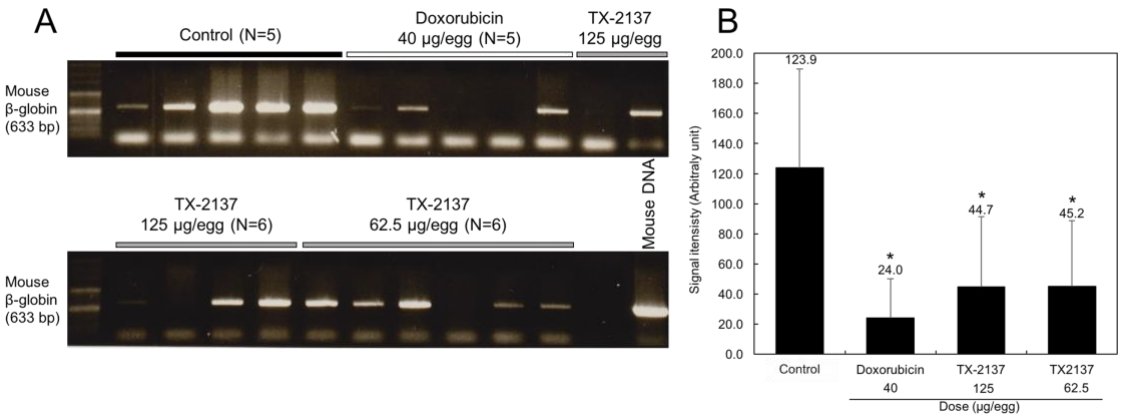

Figure 8. Evaluation of anti-metastatic activity of TX-2137 using the chick embryo model. Polymerase chain reaction analysis to detect liver metastases of B16-F10 melanoma (A) and quantitative analysis of the signal intensity shown in (A) using Image J (B). Treatment with TX-2137 and doxorubicin led to significantly lower signal intensities than that of the control (*$p<0.05$).

5. Discussion

In this chapter, I designed and synthesized TX-2137, which is a novel anti-metastatic hypoxic cytotoxin with AKT inhibitory activity, and evaluated its antitumor and anti-metastatic activities using *in vitro* and *in vivo* assay systems. TX-2137 showed strong anti-proliferative activity against tumor cell lines, with IC_{50} values ranging from 1.8 to 3.7 μM. Hypoxia-selective activity of TX-2137, however, was lower than that of tirapazamine. TX-2137 showed potent cytotoxicity even under normoxic conditions and little difference was observed compared to hypoxic conditions owing to its higher electron affinity compared with tirapazamine as shown in Figure 4. However, TX-2137 is susceptible to reduction and its reduced form may be highly cytotoxic due to hydroxyl radical production even under normoxic conditions. TX-2137 selectively down-regulated the expression of AKT2 protein and phosphorylation of AKT; these findings indicate that the 1-(4-piperidyl)-2-benzimidazolinone moiety of AKT1/2 inhibitor is not essential for its activity.

MMP9, which is a downstream target of the AKT signaling pathway, plays an important role in invasion and metastasis of various cancer types, and MMP9 has been shown to be an important molecular target for the suppression of cancer metastasis (23). HT-1080 human fibrosarcoma cells were derived from a highly metastatic tumor and produce various MMPs including MMP2, MMP3, MMP9, and MMP14/MT1-MMP (24, 25). HT-1080 cells were shown to metastasize in xenograft models using nude mouse (26) and chick embryo (27-29). In the MMP-inhibitory assay here, TX-2137 inhibited MMP9 production in HT-1080 cells. Next, I evaluated the anti-metastatic activity of TX-2137 by using the chick embryo model because the chick embryo model provides a cost-effective, easily accessible and rapid approach (30, 31). In this xenograft model, TX-2137 showed strong anti-metastatic activity against liver metastasis of B16-F10 melanoma.

From this study, TX-2137 appears to exhibit strong anti-metastatic activity through inhibition of AKT expression and phosphorylation, and suppression of MMP9 production.

6. Conclusion

In conclusion, I succeeded in the development of the anti-metastatic hypoxic cytotoxin TX-2137 possessing the inhibitory activity of AKT expression and MMP9 production (32).

7. References

[1] De Bock K, Mazzone M, Carmeliet P: Antiangiogenic therapy, hypoxia, and metastasis: risky liaisons, or not? Nat Rev Clin Oncol *31*: 393-404, 2011.

[2] Collet G, Szade K, Nowak W, Klimkiewicz K, El Hafny-Rahbi B and Szczepanek K, Sugiyama D, Weglarczyk K, Foucault-Collet A, Guichard A, Mazan A, Nadim M, Fasani F, Lamerant FN, Grillon C, Petoud S, Beloeil JC, Jozkowicz A, Dulak J and Kieda C: Endothelial precursor cell-based therapy to target the pathologic angiogenesis and compensate tumor hypoxia. Cancer Lett *370*: 345-357, 2016.

[3] Gilkes DM, Semenza GL and Wirtz D: Hypoxia and the extracellular matrix: drivers of tumour metastasis. Nat Rev Cancer *14*: 430-439, 2014.

[4] Graeber TG, Osmanian C, Jacks T, Housman DE, Koch CJ, Lowe SW and Giaccia AJ: Hypoxia-mediated selection of cells with diminished apoptotic potential in solid tumours. Nature *379*: 88-91, 1996.

[5] Muz B, de la Puente P, Azab F and Azab AK: The role of hypoxia in cancer progression, angiogenesis, metastasis, and resistance to therapy. Hypoxia Auckl *3*: 83-92, 2015.

[6] Lee C, Siu A and Ramos DM: Multicellular spheroids as a model for hypoxia-induced EMT. Anticancer Res *36*: 6259-6263, 2016.

[7] Hwang JT, Greenberg MM, Fuchs T and Gates KS: Reaction of the hypoxia-selective antitumor agent tirapazamine with a C1′-radical in single-stranded and double-stranded DNA: The drug and its metabolites can serve as surrogates for molecular oxygen in radical-mediated DNA damage reactions. Biochemistry *38*: 14248-14255, 1999.

[8] Brown JM and Wilson WR: Exploiting tumor hypoxia in cancer treatment. Nat Rev Cancer *4*: 437-447, 2004.

[9] Yin J, Glaser R and Gates KS: Electron and spin-density analysis of tirapazamine reduction chemistry. Chem Res Toxicol *25*: 620−633, 2012.

[10] Rischin D, Peters L, Fisher R, Macann A, Denham J, Poulsen M, Jackson M, Kenny L, Penniment M, Corry J, Lamb D and McClure B: Tirapazamine, cisplatin, and radiation *versus* fluorouracil, cisplatin, and radiation in patients with locally advanced head and neck cancer: A randomized phase II trial of the Trans-Tasman Radiation Oncology Group (TROG 98.02). J Clin Oncol *23*: 79-87, 2005.

[11] Williamson SK, Crowley, JJ, Lara PN Jr, McCoy J, Lau DH, Tucker RW, Mills GM and Gandara DR; Phase III trial of paclitaxel plus carboplatin with or without tirapazamine in advanced non-small-cell lung cancer: Southwest Oncology Group Trial S0003. J Clin Oncol *23*: 9097-9104, 2005.

[12] Rischin D, Peters LJ, O'Sullivan B, Giralt J, Fisher R, Yuen K, Trotti A, Bernier J, Bourhis J, Ringash J, Henke M and Kenny L: Tirapazamine, cisplatin, and radiation versus cisplatin and radiation for advanced squamous cell carcinoma of the head and neck (TROG 02.02, HeadSTART): A phase III trial of the Trans-Tasman Radiation Oncology Group. J Clin Oncol *28*: 2989-2995, 2010.

[13] Agarwal E, Brattain MG and Chowdhury S: Cell survival and metastasis regulation by AKT signaling in colorectal cancer. Cell Signal *25*: 1711-1719, 2013.

[14] King D, Yeomanson D and Bryant HE: PI3King the Lock: targeting the PI3K/AKT/mTOR pathway as a novel therapeutic strategy in neuroblastoma. J Pediatr Hematol Oncol *37*: 245-251, 2005.

[15] Almhanna K, Strosberg J and Malafa M: Targeting AKT protein kinase in gastric cancer. Anticancer Res *31*: 4387-4392, 2011.

[16] Mayer IA and Arteaga CL: The PI3K/AKT pathway as a target for cancer treatment. Annu. Rev Med *67*: 11-28, 2016.

[17] Chae YC, Vaira V, Caino MC, Tang HY, Seo JH, Kossenkov AV, Ottobrini L, Martelli C, Lucignani G, Bertolini I, Locatelli M, Bryant KG, Ghosh JC, Lisanti S, Ku B, Bosari S, Languino LR, Speicher DW and Altieri DC: Mitochondrial AKT regulation of hypoxic tumor reprogramming. Cancer Cell *30*: 257-272, 2016.

[18] Hay MP, Gamage SA, Kovacs MS, Pruijn FB, Anderson RF, Patterson AV, Wilson WR, Brown JM and Denny WA: Structure–activity relationships of 1,2,4-benzotriazine 1,4-dioxides as hypoxia-selective analogues of tirapazamine. J Med Chem *46*: 169-182, 2003.

[19] Pchalek K and Hay MP: Stille coupling reactions in the synthesis of hypoxia-selective 3-alkyl-1,2,4-benzotriazine 1,4-dioxideanticancer agents. J Org Chem *71*: 6530-6535, 2006.

[20] Sato H, Takino T, Okada Y, Cao J, Shinagawa A, Yamamoto E and Seiki M: A matrix metalloproteinase expressed on the surface of invasive tumor cells. Nature *370*: 61-65, 1994.

[21] Endo Y, Seiki M, Uchida H, Noguchi M, Kida Y, Sato H, Mai M and Sasaki T: Experimental metastasis of oncogene-transformed NIH 3T3 cells in chick embryo. Jpn J Cancer Res *83*: 274-280, 1992.

[22] Lindsley CW, Zhao Z, Leister WH, Robinson RG, Barnett SF, Defeo JD, Jones RE, Hartman GD, Huff JR, Huber HE and Duggan ME: Allosteric AKT (PKB) inhibitors: discovery and SAR of isozyme selective inhibitors. Bioorg Med Chem Lett *15*: 761-764, 2005.

[23] Itoh T, Tanioka M, Matsuda H, Nishimoto H, Yoshioka T, Suzuki R and Uehira M: Experimental metastasis is suppressed in MMP9-deficient mice. Clin Exp Metastasis *17*: 177-181, 1999.

[24] Sato H, Kida Y, Mai M, Endo Y, Sasaki T, Tanaka J and Seiki M: Expression of genes encoding type IV collagen-degrading metalloproteinases and their inhibitor TIMPs in various human tumor cells. Oncogene *7*: 77-83, 1992.

[25] Abd El-Aziz SH and Endo Y, Miyamaori H, Takino T and Sato H: Cleavage of growth differentiation factor 15 (GDF15) by membrane type 1-matrix metalloproteinase abrogates GDF15-mediated suppression of tumor cell growth. Cancer Sci *98*: 1330-1335, 2007.

[26] Ohta Y, Watanabe Y, Tabata T, Oda M, Hayashi Y, Endo Y, Tanaka M and Sasaki T: Inhibition of lymph node metastasis by an anti-angiogenic agent, TNP-470. Br J Cancer *75*: 512-515, 1997.

[27] Endo Y, Sasaki T, Harada F and Noguchi M: Specific detection of metastasized human tumor cells in embryonic chicks by the polymerase chain reaction. Jpn J Cancer Res *81*: 723-726, 1990.

[28] Tsuchiya Y, Endo Y, Sato H, Okada Y, Mai M, Sasaki T and Seiki M: Expression of type IV collagenases in human tumor cell lines that can form liver colonies in chick embryo. Int J Cancer *56*: 46-51, 1994.

[29] Li Z, Takino T, Endo Y and Sato H: Activation of matrix metalloproteinase (MMP)-9 by membrane-type-1 matrix metalloproteinase/MMP2 axis stimulates tumor metastasis. Cancer Sci *108*: 347-357, 2017.

[30] Wilson SM and Chambers AF: Experimental metastasis assays in the chick embryo. Curr Protoc Cell Biol *19*: 19.6, 2004.

[31] Uto Y, Tamatani D, Mizuki Y, Endo Y, Nakanishi I, Ohkubo K, Fukuzumi S, Ishizuka M, Tanaka T, Kuchiike D, Kubo K, Inui T and Hori H: Evaluation of the sonosensitizing activities of 5-aminolevulinic acid and Sn(IV) chlorine 6 in tumor-bearing chick embryos. Anticancer Res *34*: 4583-4587, 2014.

[32] Shiba I, Kouzaki R, Yamada H, Endo Y, Takino T, Sato H, Kitazato K, Kageji T, Nagahiro S, Uto Y: Design and Synthesis of Novel Anti-metastatic Hypoxic Cytotoxin TX-2137 Targeting AKT Kinase. Anticancer Res 37: 3877-3883, 2017.

Chapter 2: Design and Synthesis of Novel Anti-metastatic Hypoxic Cytotoxin Based on 2,3-Diphenylquinoxaline

1.Abstract

Background: Hypoxia is a characteristic of the tumor microenvironment. Cancer cells under hypoxia cause cancer malignancy such as drug resistance, radiation resistance, metastasis and invasion. AKT is expressed in human cancer cells and plays an important role in cell movement, survival and metastasis. It is known that AKT is overexpressed in hypoxic cancer cells and causes metastasis. Therefore, it is important to develop an AKT inhibitory anti-metastatic agent targeting tumor hypoxia.

Results: 2,3-diphenylquinoxaline showed anti-proliferative activity against tumor cell lines, with IC_{50} values ranging from 23.0 to 68.1 μM. However, 2,3-diphenylquinoxaline 1,4-dioxide showed not anti-proliferative activity and hypoxic cytotoxicity. In the MMP-inhibitory assay here, 2,3-diphenylquinoxaline inhibited MMP9 production in HT-1080 cells. But, 2,3-diphenylquinoxaline 1,4-dioxide not inhibited MMP9 production. Next, I evaluated the anti-metastatic activity of 2,3-diphenylquinoxaline by using the chick embryo model. 2,3-Diphenylquinoxaline showed not anti-metastatic activity against liver metastasis of B16-F10 melanoma. Compound**14** showed a few hypoxia-selective cytotoxicity as compared with 2,3-diphenylquinoxaline 1,4-dioxide.

Conclusion: 2,3-Diphenylquinoxaline can be expected as an anti-metastatic agent. However, 2,3-diphenylquinoxaline 1,4-dioxide had no anti-metastatic activity and showed no hypoxia-selective cytotoxicity. Compound **14** showed cytotoxicity compared to 2,3-diphenylquinoxaline 1,4-dioxide.

1. Introduction

In Chapter 1, I reported a novel anti-metastatic hypoxic cytotoxin TX-2137. TX-2137 showed significant results in *in vitro* and *in vivo*. By this TX-2137 showed utility of anti-metastatic hypoxic cytotoxin.

Hypoxia is a characteristic of the tumor microenvironment. Cancer cells under hypoxia are known to cause cancer malignancy such as drug resistance, radiation resistance (33,34). In tumor cells under hypoxia, metastasis is regulated leading to malignant tumor (35,36).

AKT, as known serine/threonine kinase, is expressed in many human cancer cells. AKT plays an important role in many cellular regulations including cell size proliferation, cell proliferation, survival, glucose metabolism, genome stability, angiogenesis, transcription and protein synthesis, metastasis and invasion (37-41). Activation of AKT pathway has been reported to be involved in tumor malignancy (42). Therefore, AKT is regarded as a target molecule of anti-cancer drug. To date, various AKT inhibitors have been developed (43). Among them, Ipatasertib, AZD 5363 and MK-2206 are used in clinical trials. (Figure 9). Ipatasertib is in combination with paclitaxel and the first clinical trial is being conducted on triple negative breast cancer cells in the early stages (44) (NCT02301988). AZD5336 is used in combination with oraparib in the second clinical trial, but the antitumor effect has not been reported yet (45) (NCT02576444). MK-2206 is significant results are shown in phase I in which erlotinib, carboplatin, paclitaxel and docetaxel are used in combination (46) (NCT00848718). However, in combination with erlotinib for non-small cell lung cancer, no significant results have been obtained due to side effects (47) (NCT01294306).

I focused on the structure of MK-2206, which is still undergoing clinical trials. MK-2206 has diphenylquinoxaline in the skeleton as shown by dot line (48) (Figure 10). In addition, the AKT1/2 inhibitor which is a lead compound of TX-2137 also has the similarly structure (49) (Figure 10). Therefore, I have considered that this diphenylquinoxaline has an important role in AKT inhibitory activity (Figure 10). Furthermore, it is suggested that it has hypoxic toxicity by making it an N-oxide, and it is expected to become a lead compound of anti-metastatic hypoxic cytotoxin. Anti-bacterial activity has been reported for 2,3-diphenylquinoxaline dioxide but no effect on cancer cells has been reported (50) (Figure 10)。

In this chapter, First, I evaluated whether 2,3-diphenylquinoxaline would be a candidate drug for anti-metastatic hypoxic cytotoxin. Next, I designed and synthesised of novel anti-metastatic hypoxic cytotoxin.

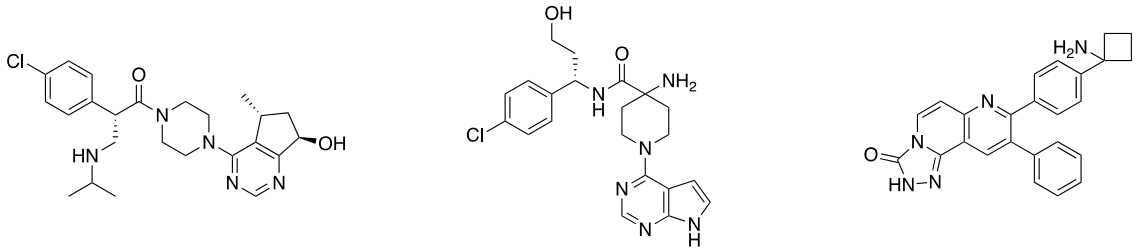

Ipatasertib AZD5363 MK-2206

Figure 9. Chemical structure of AKT inhibitor

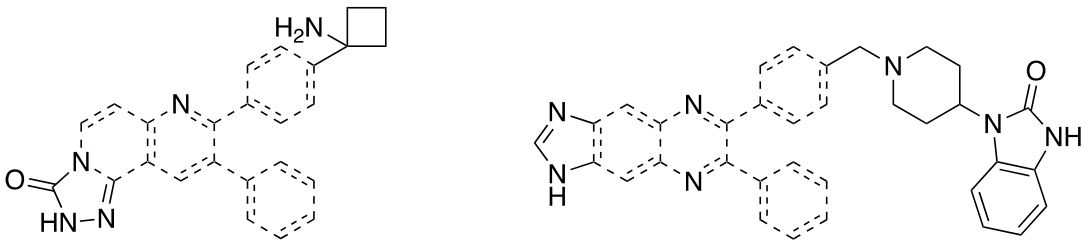

MK-2206 AKT1/2 inhibitor

2,3-Diphenylquinoxaline 2,3-Diphenylquinoxaline 1,4-dioxide

Figure 10. Structure similarly of MK-2206, AKT 1/2 inhibitor and 2,3-diphenylquinoxaline shown by dot line.

3. Materials and Methods

3-1. Materials

Reagents and solvents were purchased from standard suppliers and used without further purification unless otherwise indicated. ^{1}H nuclear magnetic resonance (NMR) spectra were obtained using a JNM-EX400 spectrometer (JEOL, Tokyo, Japan) at 400 MHz. Solvents were evaporated under reduced pressure on a rotary evaporator. Thin-layer chromatography was performed on glass-backed silica gels (Merck 60 F254; Merck Japan, Tokyo, Japan) and components were visualized using ultraviolet (UV) light. Column chromatography was performed using a silica gel (60 N, spherical neutral; 40-50 μm; KANTO Chemical, Tokyo Japan).

3-2. Cell culture

B16-F10 mouse melanoma cells (kindly provided by Dr. Tsuruo, Tokyo University, Tokyo, Japan), HT-1080 human sarcoma cells (purchased from American type culture collection, Manassas, VA, USA), PC3 human prostate cancer (purchased from American type culture collection, Manassas, VA, USA) and KKLS human undifferentiated gastric cancer cell (establishment by Dr. Asai, Kanazawa University, Kanazawa, Japan) were maintained in RPMI-1640 medium. A549 human lung carcinoma cells (supplied by Dr. Kondo, Kyoto University, Kyoto, Japan) were maintained in Dulbecco's modified Eagle's medium.

3-3. Synthesis of 2,3-diphenylquinoxaline 1,4-dioxide

o-Phenylenediamine (300 mg, 2.8 mmol) and Benzil (400 mg, 1.9 mmol) were dissolved in MeOH and reacted at room temperature for 1 h. Thereafter, the reaction was carried out at 85 ° C for 12 h. The solvents were evaporated and the residue was purified by silica-gel column chromatography with 0.5%-MeOH/CH_2Cl_2 to obtain compound **8** (524 mg, 97.7%yield) (2,3-diphenylquinoxaline). Next, 2,3-diphenylquinoxaline (200 mg, 0.7 mmol) and *m*-CPBA (368 mg, 2.1 mmol) were dissolved in CH_2Cl_2 and stirred at room temperature for 2 h. Thereafter, the reaction at reflux for 36 h. The solvents were evaporated and the residue was purified by silica-gel column chromatography with 30%-EtOAc/n-hexane to obtain compound **9** (186mg, 87.8%yield) (2,3-diphenylquinoxaline 1,4-dioxide) (15).

3-4. *In vitro* WST-8 assay to evaluate the effect of 2,3-diphenylquinoxaline and 2,3-diphenylquinoxaline 1,4-dioxide on cell proliferation

In a 96-well plate, 1 μL of compounds diluted in DMSO and serially diluted was dispensed, and 199 μL (2.5×10^4 cells / well) of a cell suspension adjusted to 2.5×10^4 cells / mL was added and cultured for 48 hours. The determination of the cell killing effect was carried out by a method using a novel tetrazolium salt WST-8 which forms water soluble formazan (Cell Counting Kit-8、DOJINDO), which is one of the MTT methods, as a chromogenic substrate. After removing the medium 72 hours after the drug treatment, 150 μL of 40-fold diluted Cell Counting Kit-8 solution was added to each well and incubated for 1 h. The produced MTT formazan was measured for absorbance at 490 nm using a microwell reader (Immunomini NJ-2300, Biotech, Tokyo).

3-5. *In vitro* hypoxia-selective cytotoxicity of 2,3-diphenylquinoxaline 1,4-dioxide using WST-1 assay

A549 cells were seeded in two 96-well plates at a density of 3×10^3 cells/well and incubation for 24 h. After 24 h, compounds were added at the final concentrations of 0.1 to 1000 μM and each plate was incubated either normoxic (21% O_2) or hypoxic (0.1% O_2) conditions for 24 h. After 24 h, each well was washed with 1×PBS and fresh medium containing the WST-1 reagent was added. The absorbance was measured at a wavelength of 450 nm using a Tecan Infinite M200 microplate reader (Tecan, Männedorf, Switzerland).

3-6. Assay of MMP9 inhibition by 2,3-diphenylquinoxaline and 2,3-diphenylquinoxaline 1,4-dioxide by gelatin zymography

10 μL of the sample (culture supernatant) was electrophoresed on a 10% polyacrylamide gel containing 0.1% gelatin. After electrophoresis, only the separated gel was cut out and shaken twice for 30 min at room temperature in the washing solution and shaken. Next, it was immersed in the reaction solution for 1 h at room temperature and shaken. Next, it was shaken while immersed in a fresh reaction solution at 37°C for 20 h. Next, the gel was shaken in a dyeing solution for 1 h at room temperature. Thereafter, the gel was shaken in a decolorizing solution for 1 h at room temperature. Finally, the gelatin decomposed (decolorized white) band was observed.

3-7. *In vivo* anti-metastatic activity of 2,3-diphenylquinoxaline using chick embryo model

Halogen light was applied to fertilized hen eggs on day 10 of incubation, marking the position and direction of blood vessels, and then removing the eggshells of the marked parts using a grinder. Liquid paraffin was added dropwise to the exposed eggshell membrane to make the blood vessels easier to view, and 0.1 ml of tumor cell suspension prepared at 1×10^6 cells / ml in the vessels of the chorioallantoic membrane was transplanted using a 30 gauge injection needle (1×10^5 cells / egg). The window of the egg after the transplant was sealed with opsite and incubated again in the incubator. On the third day after the tumor implantation (13th day of incubation), the eggshell covering the blood vessel at another position where the tumor was transplanted was removed, liquid paraffin was dropped on the exposed eggshell membrane, and using a 30 gauge injection needle 100 μL of a 10% DMSO solution of the sample was administered into the blood vessel, and incubation was carried out again in the incubator. After 7 days (17th day of incubation) after the tumor transplantation, lung and liver metastatic organs were removed from the egg fetus and the number of metastatic nodules was counted under a stereoscopic microscope.

3-8. Drug design of novel anti-metastatic hypoxic cytotoxin

2,3-Diphenylquinoxaline can be expected as an anti-metastatic agent, but N-oxide has no hypoxia selectivity and shows no anti-metastatic activity. Therefore, I designed molecular design to have hypoxic selectivity. Tirapazamine has been reported to be easily reduced due to its high electron affinity. In order to exert hypoxic toxicity, it is necessary to design N-oxide compounds with electron affinity comparable to that of Tirapazamine (Figure 11). Q 39 has been developed as a quinoxaline derivative and reported to exhibit hypoxic toxicity (Figure 11) (51). In Q 39, a part of the phenyl group is substituted with a sulfone group. In addition, it has been reported that carbonyl groups are introduced between the phenyl groups, similarly showing toxicity with hypoxia (Figure 11) (52).

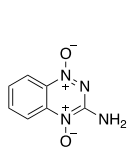

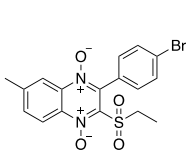

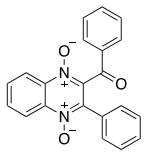

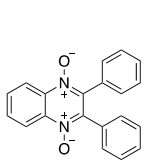

	Tirapazamine	Q39	BPQ	2,3-Diphenylquinoxaline 1,4-dioxide
LUMO (eV)	-1.4041	-2.1621	-1.4915	-5.1003
HOMO (eV)	-8.1342	-8.7900	-8.3491	-7.7996

Figure 11. Chemical structure is Hypoxic-selective drug.

3-9. Synthesis of 2-chloro-3-phenylquinoxaline 1,4-dioxide

Benzoylformic (5.0 g, 33.3 mmol) acid and *o*-phenylendiamine (3.6 g, 33.3 mmol) dissolved in Ethanol (EtOH) and stirring at 100 ˚C for 2h. After 2h, The precipitate was collected, washed with EtOH, and dried to obtain compound **10** (3-phenylquinoxalin-2(1*H*)-one) (6.8 g, 91.8%). The 3-phenylquinoxalin-2(1*H*)-one was dissolved in $POCl_3$ (70 mL) and stirred at 100 °C for 2 h. Once cooled, the solution was added dropwise to ice/water, the precipitate was collected, washed with water, and dried to obtain compound **11** (2-chloro-3-phenylquinoxaline) (7.1 g, 95.8% yield) (3,4). The 2-chloro-3-phenylquinoxaline (578 mg, 2.4 mmol) dissolved in CH_2Cl_2 and dropwise trifluoroacetic anhydride (TFAA) (7.7 mL, 48.0 mmol) on ice bath and stirring for 20 min. After 20 min, H_2O_2 (1.4 mL, 48.0 mmol) was added and stirring with reflux for 4h. The reaction solution was extracted with water and CH_2Cl_2. Organic layer was evaporated and the residue was purified by silica-gel column chromatography with 50%-EtOAc/n-hexane to obtain compound **12** (2-chloro-3-phenylquinoxaline 1,4-dioxide) (409 mg, 62.5% yield) as a yellow crystalline solid. ^{1}H NMR [$(CD_3)_2SO$] δ 8.54 (*dd*, *J* = 8.4, 1.6 Hz, 1H), 8.49 (*dd*, *J* = 8.4, 1.6 Hz, 1H), 7.97-8.05 (*m*, 2H), 7.52-7.61 (*m*, 5H).

3-10. Synthesis of compound 13

2-chloro-3-phenylquinoxaline (200 mg, 0.8 mmol) and cesium carbonate (Cs_2CO_3) (270 mg, 0.8 mmol) dissolved in DMF. Next, Thiophenol (127 μL, 1.3 mmol) was added and stirring at 70 ˚C for 48 h. After 48 h, the water was added and evaporated and the residue was purified by silica-gel column chromatography with 10%-EtOAc/n-hexane to obtain compound **13** (210 mg, 80.5%yield). ^{1}H NMR [$(CD_3)_2SO$] δ 8.04-8.06 (*m*, 1H), 7.83-7.85 (*m*, 2H), 7.72-7.76 (*m*, 2H), 7.65 (*dd*, *J* = 5.2, 4.3 Hz, 1H), 7.59-7.61 (*m*, 5H), 7.50-7.51 (*m*, 3H); MS (ESI) m/z 315 (M^+).

3-11. Synthesis of compound 14

2-chloro-3-phenylquinoxaline 1,4-dioxide (96.0 mg, 0.4 mmol) and Cs_2CO_3 (120 mg, 0.4 mmol) dissolved in DMF. Next, Thiophenol (56.0 μL, 0.6 mmol) was added and stirring at 70 ˚C for 48 h. After 48 h, the water was added and evaporated and the residue was purified by silica-gel column chromatography with 0.6%-MeOH/CH_2Cl_2 to obtain compound **14** (119 mg, 92.9%yield). ^{1}H NMR [$(CD_3)_2SO$] δ 8.52 (*d*, *J* = 8.4 Hz, 1H), 8.44 (*d*, *J* = 1.9 Hz, 1H), 7.96-8.01 (*m*, 2H), 7.45-7.49 (*m*, 5H), 7.22 (*s*, 5H); MS (ESI) m/z 347 (M^+).

3-12. Synthesis of compound 15

2-chloro-3-phenylquinoxaline (200 mg, 0.8 mmol) dissolved in Aniline (2.0 mL) and stirring at 185 ˚C for 24 h. After 24 h, HCl solution was added and CH_2Cl_2 extraction was performed. The organic layer was evaporated and the residue was purified by silica-gel column chromatography with CH_2Cl_2 to obtain compound **15** (92.0 mg, 69.7%yield). ^{1}NMR (400 MHz, DMSO-D6) δ 8.50 (s, 1H), 7.81-7.91 (m, 5H), 7.72 (dd, J = 8.0, 1.3 Hz, 1H), 7.63-7.67 (m, 1H), 7.55-7.62 (m, 3H), 7.48-7.52 (m, 1H), 7.34 (t, J = 8.0 Hz, 2H), 7.04 (t, J = 7.2 Hz, 1H); MS (ESI) m/z 298 (M^+).

3-13. Synthesis of compound 16

2-chloro-3-phenylquinoxaline 1,4-dioxide (207 mg, 0.8 mmol) and Cs_2CO_3 (490 mg, 1.6 mmol) dissolved in DMF. Next, Aniline (141 μL, 1.6 mmol) was added and stirring at 70 ˚C for 48 h. After 48 h, the solution evaporated and the residue was purified by silica-gel column chromatography with 50%-EtOAc/n-Hexane to obtain compound **16** (12 mg, 9.9%yield). ^{1}H-NMR (500 MHz, DMSO-D6) δ 12.45 (s, 1H), 8.19 (d, J = 8.4 Hz, 2H), 7.66-7.69 (m, 5H), 7.43-7.49 (m, 5H), 7.34-7.41 (m, 2H); MS (ESI) m/z 330 (M^+).

3-14. Synthesis of compound 17

2-chloro-3-phenylquinoxaline 1,4-dioxide (100 mg, 0.4 mmol) was dissolved in MeOH. 40% Methylamine in MeOH (600 μL, 7.6 mmol) and *N*,*N*-diisopropylethylamine (DIEA) (129 μL, 0.7 mmol) was added and stirring for 24 h. The solution was evaporated and the residue was purified by silica-gel column chromatography with 1%-MeOH/CH_2Cl_2 to obtain compound **17** (27 mg, 26.4%yield). ^{1}H-NMR (400 MHz, DMSO-D6) δ 8.36 (d, J = 8.7 Hz, 2H), 7.87 (t, J = 7.7 Hz, 1H), 7.73 (d, J = 5.1 Hz, 1H), 7.54-7.64 (m, 6H), 2.25 (d, J = 5.7 Hz, 3H)

3-15. Synthesis of compound 18

2-chloro-3-phenylquinoxaline (200 mg, 0.8 mmol) was dissolved in MeOH. 40% Methylamine in MeOH (797 μL, 12.5 mmol) was added and stirring for 24 h. The solution was evaporated and the residue was purified by silica-gel column chromatography with 5%-EtOAc/n-Hexane to obtain compound **18** (105 mg, 61.6%yield). ^{1}H-NMR (500 MHz, DMSO-D6) δ 7.79 (d, J = 8.4 Hz, 1H), 7.71 (q, J = 3.2 Hz, 2H), 7.64 (d, J = 8.4 Hz, 1H), 7.55-7.58 (m, 4H), 7.35 (t, J = 7.5 Hz, 1H), 6.70 (d, J = 4.5 Hz, 1H), 2.90 (d, J = 4.5 Hz, 3H).

3-16. Synthesis of compound 19

Compound **14** (60.0 mg, 0.2 mmol) and *m*-CPBA (60.0 mg, 0.3 mmol) were dissolved in CH_2Cl_2 and stirring for 24 h. The solution was evaporated and the residue was purified by silica-gel column chromatography with 10%-EtOAc/CH_2Cl_2 to obtain compound **19** (16.0 mg, 24.4%yield). ^{1}H-NMR (500 MHz, DMSO-D6) δ 8.29-8.46 (m, 2H), 7.86-8.01 (m, 2H), 7.69-7.74 (m, 2H), 7.38-7.58 (m, 8H), 3.25-3.55 (m, 16H), 2.47 (s, 4H).

3-17. *In vitro* hypoxia-selective cytotoxicity of dioxide compounds using WST-1 assay

A549 cells were seeded in two 96-well plates at a density of 3×10^3 cells/well and incubation for 24 h. After 24 h, dioxide compounds was added at the final concentrations of 0.1 to 1000 μM and each plate was incubated either normoxic (21% O_2) or hypoxic (0.1% O_2) conditions for 24 h. After 24 h, each well was washed with 1×PBS and fresh medium containing the WST-1 reagent was added. The absorbance was measured at a wavelength of 450 nm using a Tecan Infinite M200 microplate reader (Tecan, Männedorf, Switzerland).

3-18. AKT inhibition by compounds 13-19 by western blot analysis on U87MG cells

The harvested cells were homogenized in RIPA buffer (Thermo Scientific, IL, USA) supplemented with protease inhibitors (cOmplete™, Mini, EDTA-free®, Roche Applied Science Tokyo, Japan). After 5 min of centrifugation at 13000 x g, the protein concentration in the supernatant was assayed with BCA reagent (PIERCE, Tokyo, Japan). After reduction in 60 mM Tris-HCl buffer (pH 6.8) containing 10% glycerol, 2% sodium dodecyl sulfate (SDS), 100 mM dithiothreitol (DTT) and 0.002% bromophenol blue, 50 μg of protein were separated by SDS-Poly- Acrylamide Gel Electrophoresis (SDS-PAGE) and transferred to polyvinylidene fluoride (BIO-RAD, Hercules, CA, USA) membranes. The membranes were immersed for 1 h in blocking buffer [5% non-fat dry milk or 5% bovine serum albumin (BSA) in tris-buffered saline (TBS)] and then incubated with primary antibodies to AKT2, AKT3 (1:1000; Cell Signaling, Danvers, MA, USA), or phospho-AKT (Ser473) (1:2000; Cell Signaling in Can Get Signal Solution 1 (TOYOBO, Osaka, Japan). The membranes were subsequently incubated with horseradish peroxidase-conjugated secondary antibodies in Can Get Signal Solution 2 (dilution 1:3000; TOYOBO). The protein–antibody complexes were detected with Amersham ECL® plus (GE Healthcare, Little Chalfont, Buckinghamshire, UK) using a Lumino image analyzer (Image Quant LAS4000 mini; GE Healthcare) and NIH ImageJ 1.46 software (http://rsb.info.nih.gov/ij/). Each experiment was repeated three times.

4. Results

4-1. Synthesis of 2,3-diphenylquinoxaline 1,4-dioxide

2,3-Diphenylquinoxaline 1,4-dioxide was synthesized using the method described by Murthy *et al.* (Figure 12) (15).

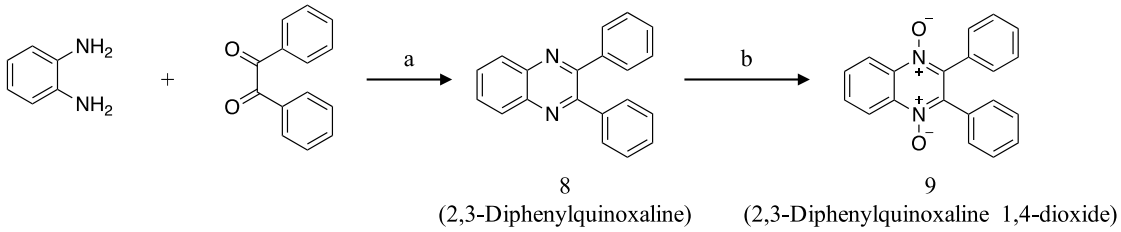

Figure 12. Synthesis of the 2,3-diphenylquinoxaline 1,4-dioxide. Reagents: a: MeOH, reflux; b: *m*-CPBA, CH_2Cl_2, reflux.

4-2. Cell proliferation-inhibitory activity and hypoxic cytotoxicity of 2,3-diphenylquinoxaline and 2,3-diphenylquinoxaline 1,4-dioxide

I first evaluated anti-proliferative activity and hypoxia-selective cytotoxicity of 2,3-diphenylquinoxaline and 2,3-diphenylquinoxaline 1,4-dioxide in different tumor cells (Table II). Table IIA shows the cell proliferation-inhibitory activity of 2,3-diphenylquinoxaline that exhibited a anti-proliferative effect against all the tumor cell lines tested. However, 2,3-diphenylquinoxaline 1,4-dioxide showed no anti-proliferative. Table IIB shows the results of the cytotoxicity assay under normoxic and hypoxic conditions. 2,3-diphenylquinoxaline 1,4-dioxide showed no hypoxic cytotoxicity.

Table II. Cell Proliferation Inhibitory Activity (A) and Hypoxic Cytotoxicity (B) of 2,3-diphenylquinoxaline and 2,3-diphenylquinoxaline 1,4-dioxide.

A

Compound	IC_{50} (μM)			
	HT-1080	KKLS	PC-3	B16-F10
2,3-diphenylquinoxaline	23.0	29.9	40.4	68.1
2,3-diphenylquinoxaline 1,4-dioxide	>200	173.0	>200	88.5

B

Compound	IC_{50} (μM) A549		Hypoxic selectivity, normoxia/hypoxia
	Normoxia	Hypoxia	
2,3-diphenylquinoxaline 1,4-dioxide	>300	>300	ND

4-3. Inhibitory activity of 2,3-diphenylquinoxaline and 2,3-diphenylquinoxaline 1,4-dioxide on MMP9 production in HT-1080 cells

The inhibitory activity of 2,3-Diphenylquinoxaline and 2,3-Diphenylquinoxaline 1,4-dioxide on MMP9 production was evaluated by zymographic assay using HT-1080 cells. 2,3-diphenylquinoxaline inhibited the production of MMP9 but did not alter MMP2 production and activation. However, 2,3-diphenylquinoxaline 1,4-dioxide not inhibited the production of MMP9 and MMP2 (Figure 13).

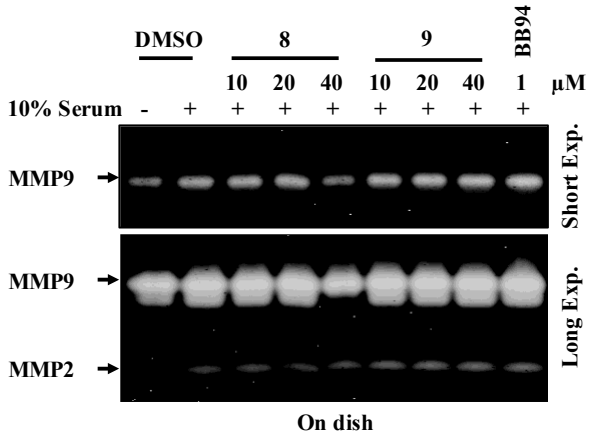

Figure 13. Effect of 2,3-diphenylquinoxaline (8) and 2,3-diphenylquinoxaline 1,4-dioxide (9) on MMP2 and MMP9. 2,3-diphenylquinoxaline inhibited expression of MMP9 in a concentration-dependent manner.

4-4. Anti-metastatic activity of 2,3-diphenylquinoxaline using chick embryo model on B16-F10 cells

Anti-metastatic activity of 2,3-diphenylquinoxaline was assayed using a xenograft model using chick embryo. 2,3-diphenylquinoxalin not effectively prevented liver metastasis of B16-F10 melanoma cells (Figure 14).

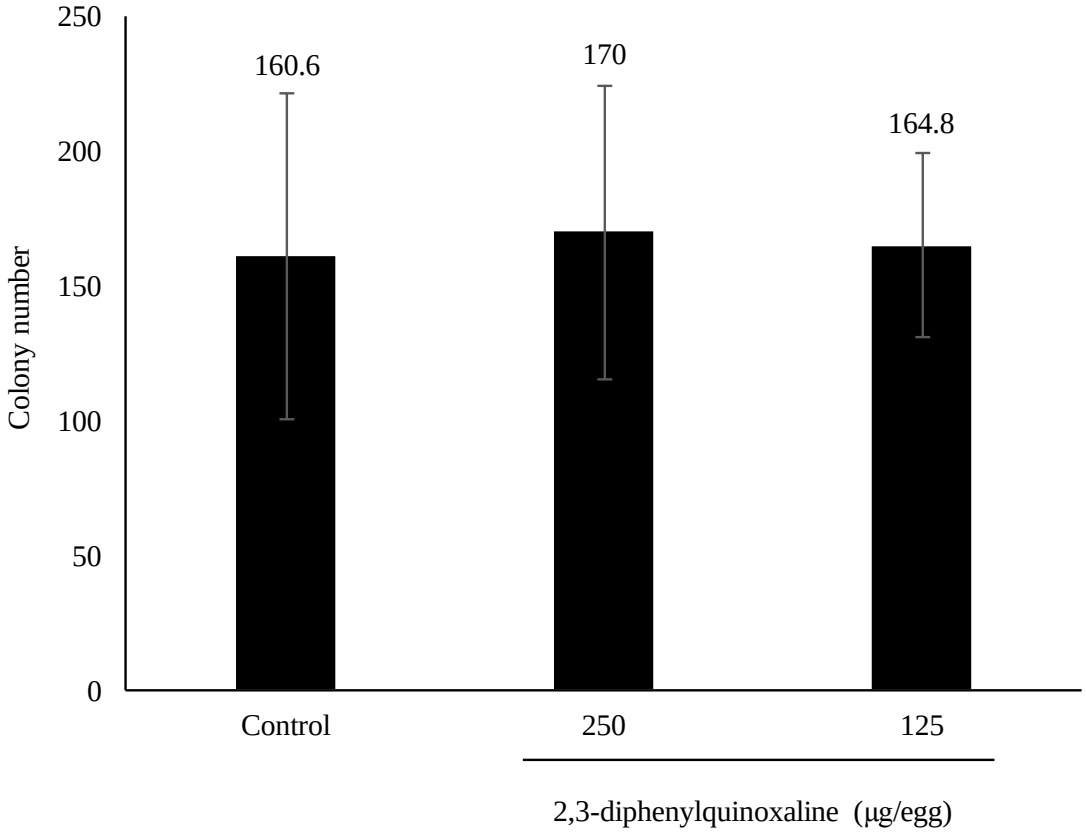

Figure 14. Evaluation of anti-metastatic activity of 2,3-diphenylquinoxaline using the chick embryo model. Count the metastatic lesion to the liver. 2,3-diphenylquinoxaline did not show anti-metastatic activity due to its low water solubility (*$p<0.05$).

4-5. Design and synthesis of novel anti-metastatic hypoxic cytotoxin

I designed of novel anti-metastatic hypoxic cytotoxin reference to Q39 and BPQ (Figure 15). 2-chloro-3-phenylquinoxaline was synthesized using the method described by Singh *et al.* and Rao *et al.* (53,54). Thereafter, the N position was oxidized to obtain 2-chloro-3-phenylquinoxaline 1,4-dioxide (Figure 16).

First, 2-chloro-3-phenylquinoxaline and tiophenol coupled to obtain compound **14** (Figure 17). Next, 2-chloro-3-phenylquinoxaline 1,4-dioxide and tiophenol coupled to obtain compound **15** (Figure 17). Similarly, coupling with aniline afforded compounds **15** and **16** (Figure 18). Next, Compounds **17** and **18** could be coupled with methylamine (Figure 19). Finally, compound **14** was oxidized to obtain compound **19** (Figure 20).

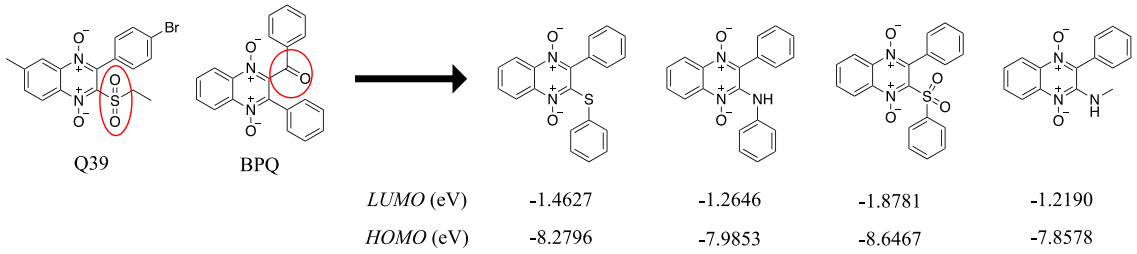

Figure 15. Design of novel anti-metastatic hypoxic cytotoxin.

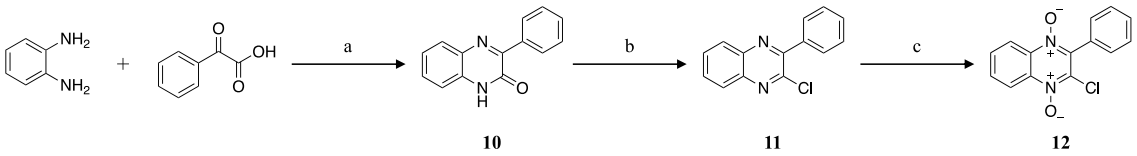

Figure 16. Synthesis of 2-chloro-3-phenylquinoxaline 1,4-dioxide. Reagents: a: EtOH, reflux; b: $POCl_3$; c: TFAA, H_2O_2, CH_2Cl_2.

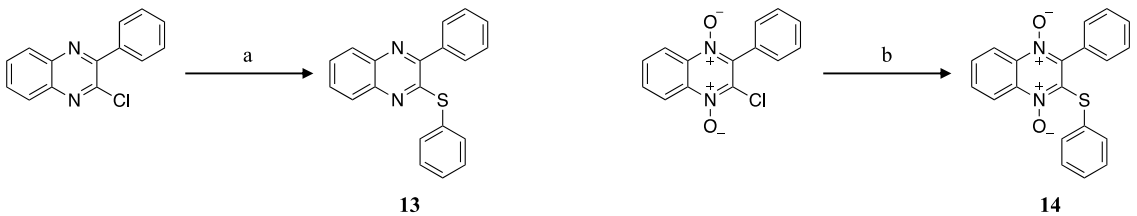

Figure 17. Synthesis of novel anti-metastatic hypoxic cytotoxin. Reagents: a: Thiophenol, Cs_2CO_3, DMF; b: Thiophenol, Cs_2CO_3, DMF.

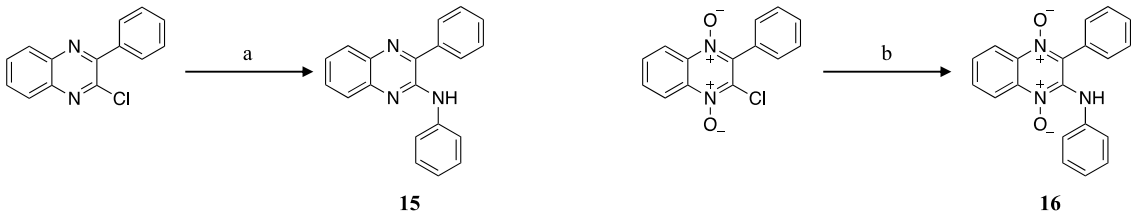

Figure 18. Synthesis of novel anti-metastatic hypoxic cytotoxin. Reagents: a: Aniline; b: Aniline, Cs_2CO_3, DMF.

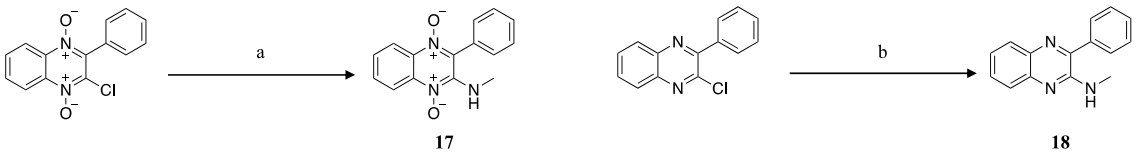

Figure 19. Synthesis of novel anti-metastatic hypoxic cytotoxin. Reagents: a: 40%-Methylamine, DIEA, MeOH; b: 40%-Methylamine, MeOH.

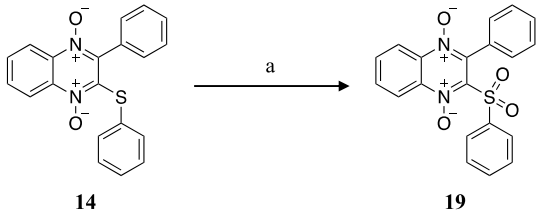

Figure 20. Synthesis of novel anti-metastatic hypoxic cytotoxin. Reagents: a: *m*-CPBA, CH_2Cl_2.

4-6. Hypoxic cytotoxicity of novel anti-metastatic hypoxic cytotoxin

I evaluated hypoxia-selective cytotoxicity and molecular orbital of dioxide compounds in A549 cells (Table III). Table I shows the results of the cytotoxicity assay under normoxic and hypoxic conditions.

Table III. Hypoxic Cytotoxicity and Molecular Orbital of Dioxide Compounds.

Compounds	IC_{50} [μM] A549			Molecular Orbital	
	Normoxia	Hypoxia	Hypoxic selectivity, normoxia/hypoxia	*HOMO*	*LUMO*
Tirapazamine	185.6	18.7	9.9	-8.1342	-1.4041
14	190.4	163.5	1.2	-8.2796	-1.4627
16	>300	>300	ND	-7.9853	-1.2646
17	318.5	631.5	ND	-7.8578	-0.219
19	15.2	12	1.3	-86467	-1.8781

4-7. AKT-inhibitory activity of compounds 13-19 on U87MG cells

I evaluated the inhibitory activity of compounds **13-19** on AKT protein expression, its phosphorylation and cell viability (Figure 21). High electron affinities compounds **14** and **19** significantly inhibited AKT phosphorylation (Figure 21A, D). In addition, compound **19** also significantly inhibited the protein of AKT2 (Figure 21B). Compound **19** effectively down-regulated the expression of AKT2,3 and the phosphorylation of AKT (Figure 21A-D).

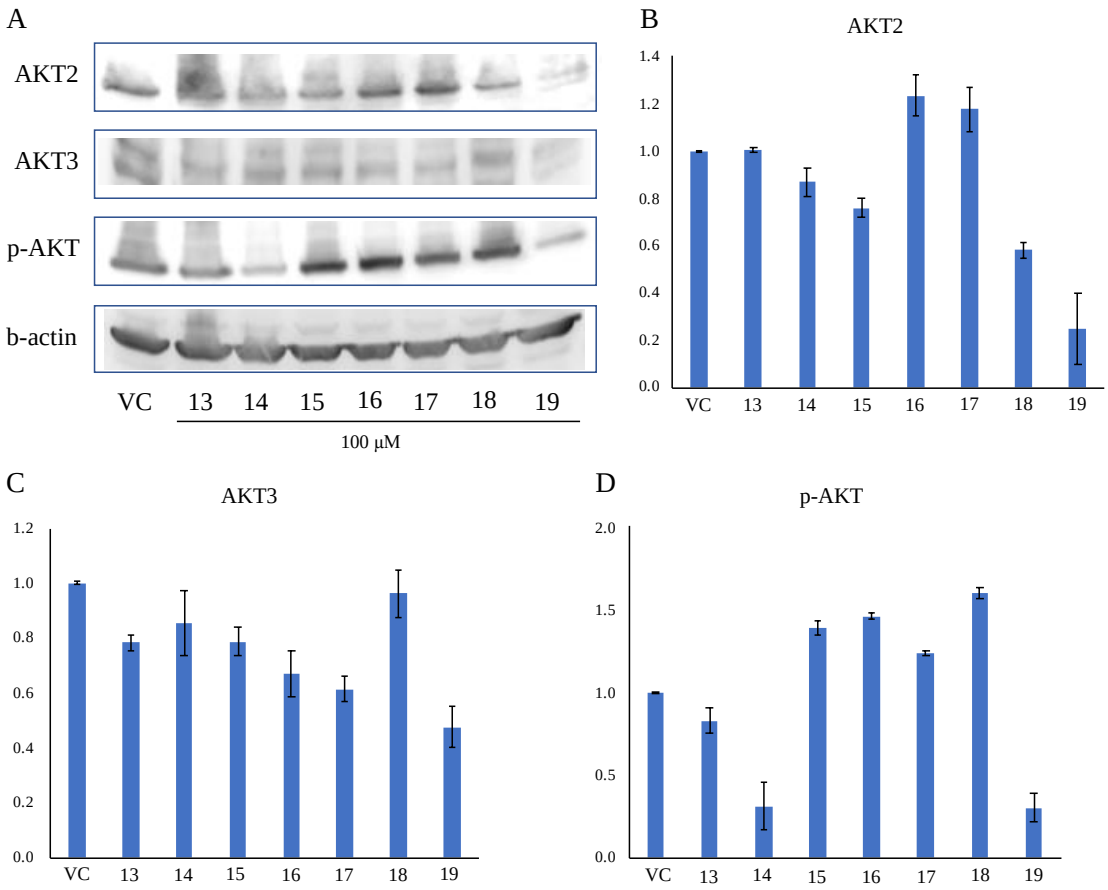

5. Discussion

In this chapter, I evaluated the anti-cancer activity of 2,3-diphenylquinoxaline and 2,3-diphenylquinoxaline 1,4-dioxide and design and synthesis of novel anti-metastatic hypoxic cytotoxin. First, 2,3-diphenylquinoxaline and 2,3-diphenylquinoxaline 1,4-dioxide evaluated using *in vitro* and *in vivo* assay. 2,3-diphenylquinoxaline showed anti-proliferative activity against tumor cell lines, with IC_{50} values ranging from 23.0 to 68.1 μM. However, 2,3-diphenylquinoxaline 1,4-dioxide showed not anti-proliferative activity and hypoxic cytotoxicity. In the MMP-inhibitory assay here, 2,3-diphenylquinoxaline inhibited MMP9 production in HT-1080 cells. But, 2,3-diphenylquinoxaline 1,4-dioxide not inhibited MMP9 production. Next, I evaluated the anti-metastatic activity of 2,3-diphenylquinoxaline by using the chick embryo model. 2,3-Diphenylquinoxaline showed not anti-metastatic activity against liver metastasis of B16-F10 melanoma. 2,3-Diphenylquinoxaline was low in water solubility and showed no significant effect in *in vivo*. Although it can ensure water solubility by setting to 2,3-diphenylquinoxaline 1,4-dioxide, it has no hypoxia selectivity and does not show anti-metastatic activity. 2,3-Diphenylquinoxaline is promising as an anti-metastatic lead compound, but in order to exhibit anti-metastatic activity *in vivo*, it is necessary to make it a dioxide compound and to have hypoxia selectivity. Therefore, anti-metastatic hypoxic cytotoxin having hypoxic toxicity and anti-metastatic activity under intracellular reduction was designed. Compounds **14** and **19** with high electron affinity showed high toxicity. Similarly, Compounds **14** and **19** inhibited phosphorylation of AKT as compared with other compounds. It was suggested that when there is a phenyl group at the 2 position, the existence of an electron-withdrawing substituent at the 3 position is susceptible to one-electron reduction.

6. Conclusion

In conclusion, 2,3-diphenylquinoxaline can be expected as an anti-metastatic agent. However, 2,3-diphenylquinoxaline 1,4-dioxide had no anti-metastatic activity and showed no hypoxia-selective cytotoxicity. Compound **14** and **19** showed cytotoxicity compared to 2,3-diphenylquinoxaline 1,4-dioxide. Compound **14** and **19** showed inhibit phosphorylation of AKT. I succeeded in the development of the AKT inhibitory hypoxic cytotoxin.

7. References

[33] Schöning JP, Monteiro M, Gu W: Drug resistance and cancer stem cells: the shared but distinct roles of hypoxia-inducible factors HIF1α and HIF2α. Clin Exp Pharmacol Physiol *44*: 153-161, 2017.

[34] Barker HE, Paget JT, Khan AA, Harrington KJ: The tumour microenvironment after radiotherapy: mechanisms of resistance and recurrence. Nat Rev Cancer 15: 409-425, 2015.

[35] Gilkes DM, Semenza GL, Wirtz D: Hypoxia and the extracellular matrix: drivers of tumour metastasis. Nat Rev Cancer 14: 430-439, 2014.

[36] Rankin EB, Giaccia AJ: Hypoxic control of metastasis. Science *352*: 175-180, 2016.

[37] DeBerardinis RJ, Lum JJ, Hatzivassiliou G, Thompson CB: The Biology of Cancer: Metabolic Reprogramming Fuels Cell Growth and Proliferation. Cell Metab *7*: 11-20, 2008

[38] Yang C, Sudderth J, Dang T, Bachoo RM, McDonald JG, DeBerardinis RJ: Glioblastoma Cells Require Glutamate Dehydrogenase to Survive Impairments of Glucose Metabolism or Akt Signaling. Cancer Res *69*: 7986-7993, 2009.

[39] Manning BD, Cantley LC: AKT/PKB Signaling: Navigating Downstream. Cell *129*: 1261-1274, 2007

[40] Karar J, Maity A: PI3K/AKT/mTOR Pathway in Angiogenesis. Front Mol Neurosci *4*: 1-8, 2011.

[41] Sheng S, Qiao M, Pardee AB: Metastasis and AKT activation. J Cell Physiol *218*: 451-454, 2009.

[42] McCubrey JA, Steelman LS, Abrams SL, Lee JT, Chang F, Bertrand FE, Navolanic PM, Terrian DM, Franklin RA, D'Assoro AB, Salisbury JL, Mazzarino MC, Stivala F, Libra M: Roles of the RAF/MEK/ERK and PI3K/PTEN/AKT pathways in malignant transformation and drug resistance. Adv Enzyme Regul *46*: 249-179, 2006.

[43] Nitulescu GM, Margina D, Juzenas P, Peng Q, Olaru OT, Saloustros E, Fenga C, Spandidos DA, Libra M, Tsatsakis AM: Akt inhibitors in cancer treatment: The long journey from drug discovery to clinical use (Review). Int J Oncol *48*: 869-885, 2016.

[44] Steven JI, Cristina S, Isabel C, Miguel J. GG, Debra AP, Serafin MM: FAIRLANE: A phase II randomized, double-blind, study of the Akt inhibitor ipatasertib (GDC-0068) in combination with paclitaxel as neoadjuvant treatment for early stage triple-negative breast cancer. J Clin Oncol *34*: 2016.

[45] Eder JP, Shapiro GI, Keedy VL: Olaparib with and without AZD1775, AZD5363, and AZD2014 in Treating Patients with Advanced Solid Tumors. NCT02576444, 2015-1017.

[46] Molife LR, Yan L, Vitfell-Rasmussen J, Zernhelt AM, Sullivan DM, Cassier PA, Chen E, Biondo A, Tetteh E, Siu LL, Patnaik A, Papadopoulos KP, de Bono JS, Tolcher AW, and Minton S: Phase 1 trial of the oral AKT inhibitor MK-2206 plus carboplatin/paclitaxel, docetaxel, or erlotinib in patients with advanced solid tumors. J Hematol Oncol *7*: 1-12, 2014.

[47] Lara PN Jr, Longmate J, Mack PC, Kelly K, Socinski MA, Salgia R, Gitlitz B, Li T, Koczywas M, Reckamp KL and Gandara DR: Phase II Study of the AKT Inhibitor MK-2206 plus Erlotinib in Patients with Advanced Non-SmallCell Lung Cancer Who Previously Progressed on Erlotinib. Clin Cancer Res 21: 4321-4326, 2015.

[48] Meuillet EJ: Novel inhibitors of AKT: assessment of a different approach targeting the pleckstrin homologydomain. Curr Med Chem *18*: 2727-2742, 2011.

[49] Lindsley CW, Zhao Z, Leister WH, Robinson RG, Barnett SF, Defeo-Jones D, Jones RE, Hartman GD, Huff JR, Huber HE and Duggan ME: Allosteric Akt (PKB) inhibitors: discovery and SAR of isozyme selective inhibitors. Bioorg Med Chem Lett *15*: 761-764, 2005.

[50] Murthya YLN, Manib P, Govindha B, Diwakara BS, Karthikeyana N, Raoc TR and Rao KVR: Synthesis and Characterization of 2,3-Diphenyl Quinoxaline 1,4-di-N-oxide Derivatives and Study of their Antimicrobial Activities.RJPBCS *2*: 553-560, 2011.

[51] Weng Q, Zhang J, Cao J, Xia Q, Wang D, Hu Y, Sheng R, Wu H, Zhu D, Zhu H, He Q and Yang B: Q39, a quinoxaline 1,4-Di-N-oxide derivative, inhibits hypoxia-inducible factor-1α expression and the Akt/mTOR/4E-BP1 signaling pathway in human hepatoma cells. Invest New Drugs 29: 1177-1187, 2011.

[52] Diab-Assef M, Haddadin MJ, Yared P, Assaad C, Gali-Muhtasib HU: Quinoxaline 1,4-dioxides: hypoxia-selective therapeutic agents. Mol Carcinog *33*: 198-205, 2002.

[53] Singh DP, Deivedi SK, Hashim SR, Singhal RG: Synthesis and Antimicrobial Activity of Some New Quinoxaline Derivatives. Pharmaceuticals (Basel) 3: 2416-2425, 2010.

[54] Rao KR, Raghunadh A, Mekala R, Meruva SB, Ganesh KR, Krishna T, Kalita D, Laxminarayana E, Pal M: Synthesis of Novel Drug-Like Small Molecules Based on Quinoxaline Containing Amino Substitution at C-2. J Heterocyclic Chem 53: 901-908, 2016.

Acknowledgement

This paper is a summary of the results of my studies enrolled in the Graduate School of Tokushima University. Dr. Uto of Professor of Tokushima University gave me the opportunity to conduct this research as an academic supervisor and received guidance from remaining all the time in carrying out the research. I show sincere gratitude here. Dr. Yamada, a lecturer from the same department, received advice and received guidance throughout the details of this thesis. I show sincere gratitude here. In the experiment of this study, Professor Sato, Associate Professor Dr. Endo and Professor Dr. Takino of Kanazawa University received materials and received valuable advice. I show sincere gratitude here. In the experiments of this study, Dr. Kitasato, Dr. Kageji and Dr. Nagahiro of Institute of Biomedical Sciences, Tokushima University Graduate School provided documents. I show sincere gratitude here. Dr. Nakamura of the technical staff gave us materials on nowadays. I show gratitude here. In our department of Uto Laboratory of members provided materials from day to day in carrying out research. I show gratitude here.